JACS
JOURNAL OF THE AMERICAN CHEMICAL SOCIETY

Communication

pubs.acs.org/JACS

Influence of Cononsolvency on the Aggregation of Tertiary Butyl Alcohol in Methanol–Water Mixtures

Kenji Mochizuki,*[,†] Shannon R. Pattenaude,[‡] and Dor Ben-Amotz[‡]

[†]Research Institute for Interdisciplinary Science, Okayama university, Okayama 700-8530, Japan

[‡]Department of Chemistry, Purdue University, West Lafayette, Indiana 47907, United States

Supporting Information

ABSTRACT: The term cononsolvency has been used to describe a situation in which a polymer is less soluble (and so is more likely to collapse and aggregate) in a mixture of two cosolvents than it is in either one of the pure solvents. Thus, cononsolvency is closely related to the suppression of protein denaturation by stabilizing osmolytes. Here, we show that cononsolvency behavior can also influence the aggregation of tertiary butyl alcohol in mixtures of water and methanol, as demonstrated using both Raman multivariate curve resolution spectroscopy and molecular dynamics simulations. Our results imply that cononsolvency results from the cosolvent-mediated enhancement of the attractive (solvophobic) mean force between nonpolar groups, driven by preferential solvation of the aggregates, in keeping with Wyman–Tanford theory.

The influence of cosolvents or osmolytes on the conformational stability of proteins and polymers[1−4] is of both fundamental interest and broad relevance to medicine and material science.[5,6] For example, the addition of an alcohol to aqueous solutions containing proteins or polymers can stabilize the folded (collapsed) state,[7,8] while high alcohol concentrations can have the opposite effect, thus inducing unfolding. Various explanations for such cononsolvency (re-entrant phase) behavior have been proposed, including Wyman–Tanford[3] and Flory–Huggins analyses,[9,10] cooperative hydrogen-bonding effects,[11] formation of alcohol/water clusters,[12,13] and preferential binding of the alcohol to the polymer.[14,15] However, the molecular origin of this phenomena remains a subject of speculation, and thus it is desirable to investigate the minimal conditions required in order to observe cononsolvency. Here we report experimental and simulation results demonstrating cononsolvency behavior in the aggregation of a small amphiphilic solute, tertiary butyl alcohol (TBA), dissolved in mixtures of water and methanol (MeOH).

Ben-Naim used the experimental solvation free energies of methane and ethane to quantify solvent-mediated contributions to a hypothetical aggregation process in which two methane molecules interpenetrate to resemble an ethane molecule, dissolved in both pure water and in ethanol/water mixtures.[16] This seminal work provided evidence of cononsolvency by revealing that solvent-mediated solvophobic interactions can be stronger in ethanol/water mixtures than in either pure water or pure ethanol. However, it is important to stress that the hypothetical methane interpenetration process is not the same as an experimental aggregation process in which two solutes come into contact with each other in solution. Very recently Mochizuki et al. used molecular dynamics (MD) simulations to demonstrate the influence of cononsolvency behavior on the formation of methane–methane direct contact aggregates in MeOH/water mixtures.[17] Whereas these prior results imply that cononsolvency arises from the cosolvent-induced enhancement of solvophobic interactions, they do not provide direct experimental evidence of cosolvent-induced aggregation of amphiphilic solute molecules. Here we provide such evidence by probing the aggregation of TBA in MeOH/water mixtures.

We chose TBA as a solute since it is one of the largest monohydric alcohols that remains infinitely miscible in water, and TBA solutions have previously been used to investigate hydrophobic hydration and interactions both theoretically[18,19] and experimentally.[20−23] Here we investigated whether the aggregation of TBA molecules is enhanced in MeOH/water mixtures by combining MD simulations and Raman multivariate curve resolution (Raman-MCR) measurements.[22−27]

We first obtained MD predictions of the potential of mean force (PMF) between a pair of TBA molecules dissolved in MeOH/water mixtures at 293 K and 0.1 MPa using two different force fields [see the caption to Figure 1, as well as the Supporting Information (SI) for further details]. Figure 1 shows the resulting TBA contact free energy (PMF minimum) as a function of

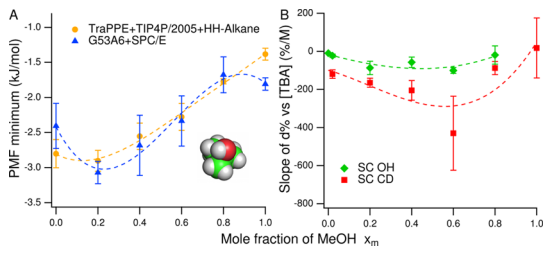

Figure 1. Dependence of intermolecular interactions between TBA (see inset structure) molecules in MeOH/water mixtures is plotted as a function of MeOH mole fraction x_m. (A) PMF contact free energy obtained using two different force fields: (orange) TraPPE[29,30] + TIP4P/2005[31] + HH-alkane,[32] and (blue) GROMOS 53A6[33] + SPC/E.[34] (B) TBA concentration-dependent slope of the solvation shell depletion (d%) for the solvent O–H (green) and C–D (red) vibrational band areas in the SC spectra of TBA in MeOH/water mixtures. Dashed lines are polynomial fits to the data points. The error bars represent either one (A) or two (B) standard deviations.

Received: May 20, 2016
Published: July 1, 2016

DOI: 10.1021/jacs.6b04914
J. Am. Chem. Soc. 2016, 138, 9045−9048

MeOH mole fraction (x_m). The results obtained using the two force fields agree in predicting that the PMF contact free energy is lowered, and thus TBA aggregation should be enhanced, when MeOH is added (up to $x_m \sim 0.2$). Both simulation results also agree in predicting that TBA should aggregate more strongly in such MeOH/water mixtures than in either pure water or pure MeOH, thus providing evidence of cononsolvency behavior. The predicted cononsolvency behavior is further supported by a Wymann–Tanford analysis (further described below, and Figure 3A) as well as by a Kirkwood–Buff integral analysis[28] (see Figure S2). Moreover, we confirm that interactions between multiple TBA molecules do not significantly affect the predicted dependence of the PMF on x_m (see Figure S3).

To experimentally test the above cononsolvency predictions, we used Raman-MCR spectroscopy to obtain solvation-shell spectra of TBA in MeOH/water mixtures[24,25] (see Experimental details in SI). Raman-MCR decomposes the measured Raman spectra of solutions into solvent (MeOH/water mixture) and solute-correlated (SC) components. Note that SC spectra may in general contain features arising from solute vibrational modes as well as any solvent molecules whose vibrational bands are perturbed by the solute. All of the SC spectra described in this work, such as those shown in Figure 2, were normalized to the

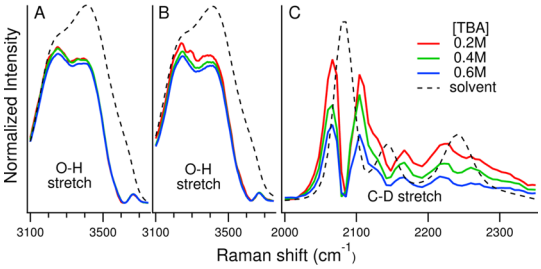

Figure 2. Pure solvent spectra (dashed curves) are compared with TBA SC spectra showing the solvent O–H (A, B) and C–D (C) vibrational bands, at TBA concentrations of 0.2 M (red), 0.4 M (green), and 0.6 M (blue). More specifically, solutions contained (A) TBA-d_9 in pure water (normalized to the same TBA-d_9 CD area) and (B, C) TBA in MeOH-d_3/water with $x_m = 0.02$ ([MeOH] ~ 1 M) (normalized to the same TBA CH area).

TBA C–H (or C–D) band area, thus effectively scaling all SC spectra to the same TBA concentration. The areas of the solvation-shell bands in such normalized SC spectra are expected to be proportional to the number of solvent molecules that are perturbed by each solute.[23] Note that the latter perturbations are expected to primarily arise from solvent molecules in the first solvation-shell around the solute. However, in a mixed solvent, the solvation-shell may also contain contributions from solvent molecules that are far from the solute if the solute significantly changes the solvent mole fraction far from the solute (as further discussed below).

To more clearly distinguish the solute and solvent methyl/methylene stretch bands, TBA was dissolved in mixtures of water and deuterated MeOH (MeOH-d_3), with $0.02 \leq x_m \leq 1.0$. The resulting SC spectrum of TBA revealed solvation-shell bands, including a C–D band arising from TBA-induced perturbations of MeOH molecules and an O–H band arising primarily from TBA-induced perturbed water molecules. Note that previous studies have demonstrated that alcohol OH head groups do not significantly contribute to Raman-MCR SC hydration-shell OH bands.[23,25] Additionally, the spectra shown in Figure 2A were obtained using deuterated TBA (TBA-d_9) dissolved in pure water, to fully separate the TBA C–D and water O–H bands, although essentially identical hydration-shell OH spectra are obtained when using nondeuterated TBA.[23] The minimum area SC spectra of C–D and O–H stretch bands were obtained by performing an MCR analysis of each of these bands independently.[25]

Figure 2 shows the SC solvation-shell O–H (A, B) and C–D (C) band spectra, obtained from (A) TBA-d_9 dissolved in pure water or (B, C) TBA in a MeOH-d_3/water mixture with $x_m = 0.02$ (which corresponds to a methanol concentration of [MeOH] ~ 1 M), with TBA concentrations varying from 0.2 to 0.6 M. Note that in pure water (Figure 2A) there is very little change in the solvation-shell O–H band area over this TBA concentration range, thus indicating that there are very few direct contacts between TBA-d_9 molecules below 0.6 M, in keeping with previous Raman-MCR, and femtosecond-IR anisotropy studies of TBA in pure water.[23] However, in the MeOH-d_3/water mixture (Figure 2B) the solvation-shell O–H band area clearly decreases with increasing TBA concentration. Such a decrease is consistent with expulsion of water molecules from the solvation-shell of TBA, resulting from TBA-TBA contacts.[23] Moreover, the SC solvation-shell C–D band of MeOH-d_3 (Figure 2C) also decreases significantly over this TBA concentration range, thus indicating that TBA aggregation also leads to a decrease in the number of MeOH-d_3 molecules that are perturbed by TBA. Similar results have been obtained in MeOH-d_3/water mixtures with x_m = 0.2, 0.4, 0.6, 0.8, 1.0 (as shown in Figure S4). These results, combined with the fact that the C–H frequency of TBA red-shifts nonlinearly as a function of x_m (see Figure S5), are all consistent with the conclusion that TBA is preferentially solvated by MeOH.

To further quantify the spectral changes shown in Figure 2, we obtained the solvation-shell depletion percentage,[23] $d\% = 100(I - I_0)/I_0$, where I is the integrated SC solvation-shell band area, and I_0 is the corresponding band area pertaining to non-aggregated TBA, obtained from the 0.1 or 0.2 M TBA solution. Thus, the slope of d% against TBA concentration is a measure of the magnitude of aggregation-induced depletion of the TBA solvation-shell and is thus also expected to reflect the degree of TBA aggregation. The points in Figure 1B show this TBA concentration-dependent slope of d% obtained from SC solvation-shell O–H (green) and C–D (red) band areas, plotted as a function of x_m. (The d%s as a function of TBA concentration are shown in Figure S6.) The minimum in these plots again provides evidence of cononsolvency, as it implies that TBA aggregates more significantly in MeOH-d_3/water mixtures than in either pure water or pure MeOH-d_3. However, in contrast to the MD predictions shown in Figure 1A, which attain a minimum at $x_m \sim 0.2$, the experimental Raman-MCR results shown in Figure 1B imply that aggregation is most strongly enhanced at a higher MeOH mole fraction $x_m \sim 0.6$.

It is not yet clear if the discrepancy between the MD and experimental results is due to shortcomings of the classical MD potential functions or shortcomings in the interpretation of the experimental Raman-MCR results obtained from three component mixtures containing a solute in solvent mixture. More specifically, note that in a two-component system, such as TBA in pure water, the Raman-MCR solvation-shell spectrum must arise from water molecules near TBA, as water molecules far from TBA must resemble bulk water. However, in a three-component mixture TBA may in principle perturb the solvent mole fraction both near and far from the solute. Thus, although we expect that the observed SC spectral perturbations are primarily from the

DOI: 10.1021/jacs.6b04914
J. Am. Chem. Soc. 2016, 138, 9045–9048

local solvation-shell around TBA, they may also contain contributions from solute-induced changes in the MeOH mole fraction far from TBA. Although it is not yet clear whether such perturbations may contribute to the observed discrepancy between the location of the minima in Figure 2A,B, both the MD and experimental results agree in indicating that the initial addition of MeOH to water leads to an enhancement of TBA aggregation.

In an effort to further elucidate the mechanism responsible for the observed cononsolvency, we performed a Wyman−Tanford preferential binding analysis[3,35,36] of our MD simulation results. The central parameter in Wyman−Tanford theory is the preferential binding coefficient Γ of the cosolvent (MeOH) to the solute (TBA) expressed as follows:

$$\Gamma = \left\langle n_m - \frac{N_m - n_m}{N_w - n_w} n_w \right\rangle$$

where n_i is the number of molecules of type i (i = m for MeOH and i = w for water) that are bound to TBA, N_i is the total number of molecules of type i, and the angle brackets $\langle \cdots \rangle$ represent an ensemble average. Thus, Γ represents the magnitude of differential affinity of MeOH and water for TBA, such that Γ is positive if the mole fraction of MeOH in the vicinity of TBA is higher than the mole fraction of MeOH in the solvent. Furthermore, the conformational equilibrium constant (K) between two different states (denoted as 1 and 2) of the solute is predicted to depend on the difference between the corresponding Γ values, where a_m is the cosolvent (MeOH) activity.

$$\frac{\partial \ln K_{1\to 2}}{\partial \ln a_m} = \Gamma_2 - \Gamma_1 \quad (1)$$

We performed MD simulations to obtain the predicted Γ for two TBA monomers (1) and one TBA dimer (2) dissolved in MeOH/water mixtures of x_m = 0.2 and 0.8 using umbrella samplings. Although Γ in general pertains to the preferential solvation integrated out to an arbitrarily large distance from the solute, we expect that the influence of a cosolvent is primarily local and thus computed Γ as a function of the cutoff distance (r) from a TBA molecule. More specifically, we define r as the shortest distance between the center carbon of either TBA and the MeOH carbon (to compute n_m), or the water oxygen (to compute n_w). Figure 3A shows Γ predictions obtained using the force field of GROMOS 53A6 and SPC/E, which is also used for the analyses in Figure 4. The results in Figure 3A indicate that the

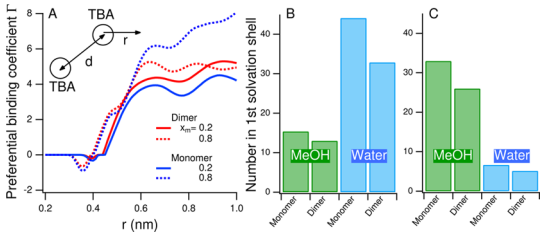

Figure 3. (A) The preferential binding coefficients for the TBA dimer (Γ_2) and monomer (Γ_1) as a function of the cutoff distance r, where the intermolecular distance (d) of TBA molecules is constrained at 0.6 nm (a dimer) and 1.6 nm (two monomers). The left top figure schematically describes the distances of d and r. Average number of MeOH and water molecules in the first solvation shell (r < 0.67 nm) around two TBA monomers and a TBA dimer (B) at x_m = 0.2 and (C) at x_m = 0.8.

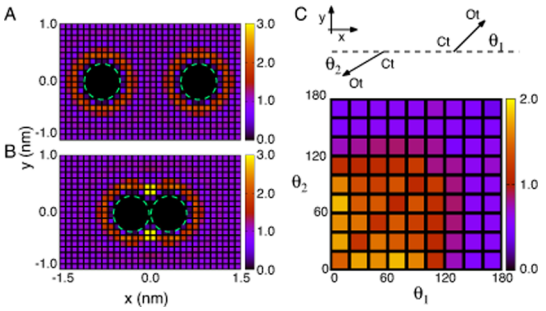

Figure 4. (A) Normalized distribution function of MeOH density at x_m = 0.2 in the vicinity of two TBA monomers and (B) a TBA dimer. The contour value of 1.0 represents the bulk MeOH density. The x and y axes are horizontal and vertical, respectively, to a straight line between center carbon atoms of the two TBA molecules. (C) Normalized orientation distribution (θ_1, θ_2) of a TBA dimer, at x_m = 0.2, with respect to a random distribution (which is proportional to sin θ_1 · sin θ_2). The top right figure indicates how θ_1 and θ_2 are related to the locations of the TBA oxygen (Ot) and center carbon (Ct) atoms.

Γ values for monomer (1) and dimer (2) structures are both positive over the entire range of r up to 1.0 nm (except in a very small region near r = 0.4 nm). The positive sign indicates that MeOH preferentially binds to both the TBA monomer and dimer structures, which are also seen in Figure 4A,B. These results clearly indicate that the magnitude of Γ for the dimer is invariably larger than that for monomer ($\Gamma_2 > \Gamma_1$) at x_m = 0.2, while $\Gamma_2 < \Gamma_1$ at x_m = 0.8. According to eq 1, $\Gamma_2 > \Gamma_1$ implies that the dimer population increases upon addition of MeOH at x_m = 0.2, while the monomer population increases upon addition of MeOH at x_m = 0.8 (and results at other values of x_m are provided in Figure S7). Thus, these Wyman−Tanford results are consistent with the x_m dependence of TBA-TBA PMF minimum shown in Figure 1A.

Further insight into the preferential solvation process may be obtained from the MD analyses for the average number of MeOH and water molecules in the first solvation shell of TBA, as obtained by counting the average number molecules within r < 0.67 nm (the first minimum of the radial distribution function between the carbon of MeOH and the center carbon of TBA at x_m = 0.2). Figure 3B,C shows how the number of MeOH and water molecules in the solvation-shells of a pair of TBA molecules change upon dimerization of TBA at x_m = 0.2 and 0.8. In both cases, the number of MeOH and water molecules decreases upon TBA dimerization (because they are excluded from the contact region between two TBA molecules). However, MeOH is less excluded than water at x_m = 0.2, while MeOH is more excluded than water at x_m = 0.8, in keeping with the Wymann−Tanford prediction that $\Gamma_2 > \Gamma_1$ at x_m = 0.2 and $\Gamma_2 < \Gamma_1$ at x_m = 0.8.

The simulation results shown in Figure 4 provide further insight into the structure of the TBA solvation-shell as well as the relative orientations of dimerized TBA molecules. The MeOH concentration contour plots in panels (A) and (B) reveal the enhanced concentration of bridging MeOH molecules (yellow domains) in the vicinity of TBA contacts. Moreover, panel (C) shows that contacting TBA molecules are oriented preferentially with their methyl groups toward each other. Qualitatively similar (but quantitatively different) results are obtained using the two different sets of potential functions.

Comparison of the results in Figures 2B,C and 3B reveals another apparent discrepancy between the experimental and MD

DOI: 10.1021/jacs.6b04914
J. Am. Chem. Soc. 2016, 138, 9045−9048

results. More specifically, the experimental Raman-MCR solvation-shell depletion results imply that dimerization leads to a greater solvation-shell depletion of MeOH than water, while the MD results imply that water is more strongly depleted than MeOH. Although the explanation for this discrepancy is not yet clear, the following possible explanation is qualitatively consistent with both experimental observations and MD predictions. In particular, the large solvation-shell depletion of MeOH shown in Figure 2C may result from MeOH molecules located at the hydrophobic end of TBA, near its three methyl groups. Upon TBA aggregation, these perturbed MeOH molecules should be displaced and thus move either to another region of the solvation-shell or out to the solvent. Thus, the large depletion of MeOH observed using Raman-MCR may reflect the displacement of these particular MeOH molecules from the hydrophobic end of TBA to some other part of the TBA solvation-shell, in keeping with the results in Figures 3B and 4C.

In summary, we find that the cononsolvency behavior appears even for small amphiphilic molecules dissolved in MeOH/water mixtures, as TBA aggregation is more pronounced in MeOH/water mixtures than in either pure MeOH or pure water, although we do not find any evidence of a phase change or microheterogeneity, e.g., clouding or liquid−liquid phase separation. These results combined with earlier studies[16,17] imply that the nonpolar groups of TBA may play a dominant role for the enhanced aggregation of TBA in MeOH/water mixtures. The Wyman−Tanford analysis further suggests that the observed cononsolvency results from the preferential binding of MeOH to the dimer of TBA as opposed to the two separated TBA monomers. In other words, our results suggest that the enhanced aggregation of TBA in MeOH/water mixtures is linked to the fact that TBA molecules prefer to reside in MeOH-rich domains. Although the MD and experimental results are in general agreement, it is not yet clear if the remaining discrepancies are due to inaccuracies in the simulation potential functions or inaccuracies in the interpretations of the experimental Raman-MCR results. To further understand the molecular origin of cononsolvency, it would be useful to further explore inhomogeneous mixing in the MeOH/water solvent itself,[37,38] as well as to determine whether other osmolytes affect the aggregation of small solutes in a way that is similar to their effect on protein folding and denaturation.

■ ASSOCIATED CONTENT

Supporting Information

The Supporting Information is available free of charge on the ACS Publications website at DOI: 10.1021/jacs.6b04914.

Computational and experimental details (PDF)

■ AUTHOR INFORMATION

Corresponding Author

*mochizuki@okayama-u.ac.jp

Notes

The authors declare no competing financial interest.

■ ACKNOWLEDGMENTS

K.M. was supported by JSPS KAKENHI, grant no. 15H05474, and the program for promoting the enhancement of research universities, MEXT, Japan. S.R.P. and D.B.-A. were supported by the National Science Foundation, grant no. CHE-1464904. Most of the calculations were performed at the Research Center for Computational Science in Okazaki, Japan, and the experiments were performed in the Department of Chemistry at Purdue University.

■ REFERENCES

(1) Scherzinger, C.; Schwarz, A.; Bardow, A.; Leonhard, K.; Richtering, W. *Curr. Opin. Colloid Interface Sci.* **2014**, *19*, 84.
(2) Timasheff, S. N. *Proc. Natl. Acad. Sci. U. S. A.* **2002**, *99*, 9721.
(3) Mondal, J.; Halverson, D.; Li, I. T. S.; Stirnemann, G.; Walker, G. C.; Berne, B. J. *Proc. Natl. Acad. Sci. U. S. A.* **2015**, *112*, 9270.
(4) Sagle, L. B.; Zhang, Y.; Litosh, V. A.; Chen, X.; Cho, Y.; Cremer, P. S. *J. Am. Chem. Soc.* **2009**, *131*, 9304.
(5) Ward, M. A.; Georgiou, T. K. *Polymers* **2011**, *3*, 1215.
(6) de Beer, S.; Kutnyanszky, E.; Schön, P. M.; Julius Vancso, G.; Müser, M. H. *Nat. Commun.* **2014**, *5*, 3781.
(7) Winnik, F. M.; Ringsdorf, H.; Venzmer, J. *Macromolecules* **1990**, *23*, 2415.
(8) Zhang, G.; Wu, C. *Phys. Rev. Lett.* **2001**, *86*, 822.
(9) Amiya, T.; Hirokawa, Y.; Hirose, Y.; Li, Y.; Tanaka, T. *J. Chem. Phys.* **1987**, *86*, 2375.
(10) Schild, H. G.; Muthukumar, M.; Tirrell, D. A. *Macromolecules* **1991**, *24*, 948.
(11) Tanaka, F.; Koga, T.; Winnik, F. M. *Phys. Rev. Lett.* **2008**, *101*, 028302.
(12) Zhang, G.; Wu, C. *J. Am. Chem. Soc.* **2001**, *123*, 1376.
(13) Pang, J.; Yang, H.; Ma, J.; Cheng, R. *J. Phys. Chem. B* **2010**, *114*, 8652.
(14) Rodríguez-Ropero, F.; Hajari, T.; van der Vegt, N. F. A. *J. Phys. Chem. B* **2015**, *119*, 15780.
(15) Mukherji, D.; Marques, C. M.; Kremer, K. *Nat. Commun.* **2014**, *5*, 4882.
(16) Ben-Naim, A. *Hydrophobic Interactions*; Springer: New York, 1980.
(17) Mochizuki, K.; Koga, K. *Phys. Chem. Chem. Phys.* **2016**, *18*, 16188.
(18) Shulgin, I. L.; Ruckenstein, E. *Phys. Chem. Chem. Phys.* **2008**, *10*, 1097.
(19) Gupta, R.; Patey, G. N. *J. Chem. Phys.* **2012**, *137*, 034509.
(20) Bowron, D. T.; Finney, J. L. *Phys. Rev. Lett.* **2002**, *89*, 215508.
(21) Subramanian, D.; Boughter, C. T.; Klauda, J. B.; Hammouda, B.; Anisimov, M. A. *Faraday Discuss.* **2014**, *167*, 217.
(22) Wilcox, D. S.; Rankin, B. M.; Ben-Amotz, D. *Faraday Discuss.* **2014**, *167*, 177.
(23) Rankin, B.; Ben-Amotz, D.; van der Post, S. T.; Bakker, H. J. *J. Phys. Chem. Lett.* **2015**, *6*, 688.
(24) Perera, P.; Wyche, M.; Loethen, Y.; Ben-Amotz, D. *J. Am. Chem. Soc.* **2008**, *130*, 4576.
(25) Davis, J. G.; Gierszal, K. P.; Wang, P.; Ben-Amotz, D. *Nature* **2012**, *491*, 582.
(26) Davis, J. G.; Rankin, B. M.; Gierszal, K. P.; Ben-Amotz, D. *Nat. Chem.* **2013**, *5*, 796.
(27) Long, J. A.; Rankin, B. M.; Ben-Amotz, D. *J. Am. Chem. Soc.* **2015**, *137*, 10809.
(28) Mochizuki, K.; Sumi, T.; Koga, K. *Sci. Rep.* **2016**, *6*, 24657.
(29) Martin, M. G.; Siepmann, J. I. *J. Phys. Chem. B* **1998**, *102*, 2569.
(30) Martin, M. G.; Siepmann, J. I. *J. Phys. Chem. B* **1999**, *103*, 4508.
(31) Abascal, J. L. F.; Vega, C. *J. Chem. Phys.* **2005**, *123*, 234505.
(32) Ashbaugh, H. S.; Liu, L.; Surampudi, L. N. *J. Chem. Phys.* **2011**, *135*, 054510.
(33) Oostenbrink, C.; Villa, A.; Mark, A. E.; van Gunsteren, W. F. *J. Comput. Chem.* **2004**, *25*, 1656.
(34) Berendsen, H. J. C.; Grigera, J. R.; Straatsma, T. P. *J. Phys. Chem.* **1987**, *91*, 6269.
(35) Wyman, J. J. *Adv. Protein Chem.* **1964**, *19*, 223.
(36) Tanford, C. *J. Mol. Biol.* **1969**, *39*, 539.
(37) Dixit, S.; Crain, J.; Poon, W. C. K.; Finney, J. L.; Soper, A. K. *Nature* **2002**, *416*, 829.
(38) Nagasaka, M.; Mochizuki, K.; Leloup, V.; Kosugi, N. *J. Phys. Chem. B* **2014**, *118*, 4388.

DOI: 10.1021/jacs.6b04914
J. Am. Chem. Soc. 2016, 138, 9045−9048